DGfM

Two new root endophyte and nematode cyst parasite species of the widely distributed genus *Laburnicola*

Dániel G. Knapp[1] · Galiya K. Akhmetova[1] · Gábor M. Kovács[1,2] · Abdelfattah A. Dababat[3] · Wolfgang Maier[4] · Samad Ashrafi[4]

Abstract

Fungal root endophytes, including the common form group of dark septate endophytes (DSEs), represent different taxonomic groups with potentially diverse life strategies. During surveys of DSE communities and of nematode cysts colonizing fungi, isolates representing *Laburnicola* (*Didymosphaeriaceae*, *Pleosporales*) lineages were discovered. Here we carried out a comprehensive study of the phylogenetic relationships and taxonomy of fungi collected from plant roots in Hungary, Mongolia, and Kazakhstan and from eggs of the cereal cyst nematode *Heterodera filipjevi* in Turkey. In addition to the study of the morphology and culture characteristics of the strains, four loci (internal transcribed spacer, partial large and small subunit regions of nuclear ribosomal DNA and partial translation elongation factor 1-alpha) were used to infer the molecular phylogenetic relationships of the strains within *Laburnicola*. The isolates were found to represent two distinct lineages, which are described here as novel species, *Laburnicola nematophila* and *L. radiciphila*. The interaction of the strains with plants and nematodes was examined using in vitro bioassays, which revealed endophytic interactions with the plant roots and parasitic interactions with the nematode eggs. Analyses of similar ITS sequences found in public databases revealed that members of the genus *Laburnicola* are widely distributed characteristic members of the plant microbiome, and they are reported as parasites of plant parasitic cyst nematodes here for the first time.

Introduction

Healthy roots of terrestrial plants host a plethora of various microorganisms, including fungal endophytes, which colonize plant tissues during some period of their life cycle, yet cause no symptoms of tissue damage to their hosts (Petrini 1991; Saikkonen et al. 1998; Schulz and Boyle 2005). A common form group of these root-associated non-mycorrhizal fungi is the so-called dark septate endophytes (DSEs) that are characterized by mainly melanized septate hyphae and microsclerotia (Jumpponen and Trappe 1998; Sieber and Grünig 2013). These fungi are common members of the root microbiome, and seem to be especially frequent in certain environments, e.g., in grasslands. Their role in the ecosystem and their effects on host plants are still enigmatic (Mandyam and Jumpponen 2005; Newsham 2011; Porras-Alfaro and Bayman 2011; Mayerhofer et al. 2013; Sieber and Grünig 2013). Recent findings of

---

Wolfgang Maier and Samad Ashrafi are joint senior authors.

Section Editor: Roland Kirschner

✉ Dániel G. Knapp
danielgknapp@ttk.elte.hu

✉ Samad Ashrafi
samad.ashrafi@julius-kuehn.de

[1] Department of Plant Anatomy, Institute of Biology, Eötvös Loránd University, Pázmány Péter sétány 1/C, Budapest 1117, Hungary

[2] Centre for Research, Plant Protection Institute, Eötvös Loránd Research Network, Budapest, Hungary

[3] International Maize and Wheat Improvement Center (CIMMYT), P.O. Box 39, Emek, 06511 Ankara, Turkey

[4] Institute for Epidemiology and Pathogen Diagnostics, Julius Kühn Institute (JKI) – Federal Research Centre for Cultivated Plants, Messeweg 11/12, 38104 Braunschweig, Germany

🖄 Springer

comparative genomics revealed an expansion of carbohydrate-active enzyme families in DSEs (Knapp et al. 2018) suggesting that the saprobic capacity of DSEs might play an important role in their interaction with the plants and the ecosystem (Knapp and Kovács 2016; Németh et al. 2022).

Plant parasitic nematodes are in direct contact with the roots of host plants and it has been shown that several nematophagous fungi can colonize plant roots asymptomatically (Bordallo et al. 2001). The DSE fungi that are present in these infected roots can improve the defense of plants against nematodes and may provide nutritional benefits to the host (Rodriguez et al. 2009; Barelli et al. 2016; Schouten 2016). However, to date, *Polyphilus sieberi* is the only known nematode egg-parasitic fungus that is also a well-characterized DSE colonizing the roots of various plant species as well as the fruiting bodies of truffles (Ashrafi et al. 2018).

DSEs represent many ascomycetous orders; however, the majority belongs to *Helotiales* (*Leotiomycetes*) and *Pleosporales* (*Dothideomycetes*) (Andrade-Linares and Franken 2013; Sieber and Grünig 2013; Jumpponen et al. 2017). The order *Helotiales* comprises many DSE fungi (Sieber and Grünig 2013), among them for example the well-known *Cadophora* species (Knapp et al. 2018) and the *Phialocephala fortinii* s.l.–*Acephala applanata* species complex (PAC) (Grünig et al. 2008), or the enigmatic genus *Polyphilus* with a host range spanning the three kingdoms of plants, fungi, and animals (Ashrafi et al. 2018). The order *Pleosporales* accommodates frequent and widely distributed members of DSEs, especially of grasslands (Sieber and Grünig 2013; Jumpponen et al. 2017; Knapp et al. 2012, 2019), e.g., *Periconia macrospinosa*, the diverse species of the genus *Darksidea* and further species mainly representing the suborders *Pleosporineae* and *Massarineae* (Mandyam et al. 2010; Knapp et al. 2015, 2018; Sieber and Grünig 2013; Romero-Jiménez et al. 2022). The family *Didymosphaeriaceae* is a well-supported monophyletic group within the *Massarineae* (Tanaka et al. 2015; Yuan et al. 2020). It accommodates many saprobic fungi, while other species are endophytes or pathogens associated with a wide variety of plants worldwide (Liu et al. 2015). Ariyawansa et al. (2014) synonymized *Montagnulaceae* under *Didymosphaeriaceae*, and this family now comprises two genera (*Alloconiothyrium* and *Paraconiothyrium*) with asexual species and 31 genera with known sexual morphs, namely, *Austropleospora*, *Barria*, *Bimuria*, *Chromolaenicola*, *Curreya*, *Cylindroaseptospora*, *Deniquelata*, *Didymocrea*, *Didymosphaeria*, *Kalmusia*, *Kalmusibambusa*, *Karstenula*, *Laburnicola*, *Letendraea*, *Lineostroma*, *Montagnula*, *Neokalmusia*, *Neptunomyces*, *Paracamarosporium*, *Paramassariosphaeria*, *Paraphaeosphaeria*, *Phaeodothis*, *Pseudocamarosporium*, *Pseudodidymocyrtis*, *Pseudopithomyces*, *Pseudotrichia*, *Spegazzinia*, *Tremateia*, *Verrucoconiothyrium*, *Vicosamyces*, and *Xenocamarosporium* (Wijayawardene et al. 2014, 2022; Liu et al. 2015; Tanaka et al. 2015; Wanasinghe et al. 2016; Yuan et al. 2020).

The genus *Laburnicola* in *Didymosphaeriaceae* was originally described with four species: *Laburnicola centaurea*, *L. dactylidis*, *L. hawksworthii*, and *L. muriformis* (Wanasinghe et al. 2016). Those four species were found on the stems of different plants in Italy and they were morphologically characterized by their sexual morphs (Wanasinghe et al. 2016). Later, *L. halophila* was described from a halophytic plant as a DSE forming only thalloconidia and no ascomata (Yuan et al. 2020). A sixth species, *L. zaaminensis*, was described and morphologically characterized by its asexual morph (Htet et al. 2021). These six *Laburnicola* species formed a monophyletic, well-supported clade in multi-locus phylogenetic analyses (Htet et al. 2021).

During investigations of root endophytes of grasslands of the Eurasian steppe belt in Hungary, Mongolia, and Kazakhstan (Knapp et al. 2012, 2019; Akhmetova et al. 2021, 2022), we have regularly isolated fungi phylogenetically representing the genus *Laburnicola*. Ever since the first isolate was found on *Festuca vaginata* in a semiarid sandy grassland of Hungary ('group-11' sensu Knapp et al. 2012), many additional isolates representing *Laburnicola* lineages from healthy roots of mainly gramineous plants were isolated (Knapp et al. 2019; Akhmetova et al. 2022). Also, numerous sequences can be found in public databases, which probably represent distinct *Laburnicola* lineages. Further strains with high sequence similarity to *Laburnicola* sequences were also isolated from eggs of the cereal cyst nematode (CCN) *Heterodera filipjevi* from the Central Anatolian Plateau of Turkey. Based on the isolation sources, these fungi resembled the isolation of *Polyphilus sieberi*, which was also identified independently from the roots of several plant species, nematode eggs and cysts and the ascomata of a truffle (Ashrafi et al. 2018).

Here, we studied isolates obtained from both the roots of different plants and from the eggs of *H. filipjevi*. The results of the initial DNA barcoding using ITS sequences showed that those isolates represented the genus *Laburnicola*, and the lineages they formed were distinct from the known species of the genus. To determine their phylogenetic relationships and clarify their taxonomy, our aims were to (i) carry out multi-locus phylogenetic analyses and morphological studies and describe the potential novel species and to (ii) conduct in vitro resynthesis experiments with plants and nematodes to gain insights into their interaction to better understand their potential roles in the ecosystem.

Materials and methods

Sampling and isolation of fungal strains

Nine fungal isolates originating from different hosts and geographic regions were examined in the present study (Table 1).

Five of these were isolated from healthy plant roots originating from Hungary, Mongolia, and Kazakhstan (isolation method as described in Knapp et al. 2012). Four isolates were obtained from symptomatic eggs of the plant parasitic nematode *Heterodera filipjevi* collected from wheat fields in the Central Anatolian Plateau of Turkey (isolation method as described in Ashrafi et al. 2017). The holotype specimens of the novel taxa were dried and deposited as metabolically inactive samples in the herbarium of the Hungarian Natural History Museum, Budapest, under the accession numbers 111910BP and 111911BP. Ex-type and other cultures were deposited in the German Collection of Microorganisms and Cell Cultures GmbH (DSMZ, Braunschweig, Germany) under the accession numbers DSM 112861–DSM 112868. Nomenclatural novelties and descriptions were registered at MycoBank (www. MycoBank.org, Crous et al. 2004).

Fungal growth, morphology, and sporulation

Four replicates of each of the nine isolates were sub-cultured onto potato dextrose agar (PDA) and corn meal agar (CMA) media (4-mm-diameter fungal plugs onto 9-cm Petri dishes). Growth rate and colony characteristics were recorded after cultures were grown for 3 weeks at temperatures from 5 to 35 °C at 5 °C intervals in the dark. The isolates that survived growing at 35 °C were additionally incubated at 37 and 40 °C for 4 weeks. To induce sporulation, the isolates were also cultured on autoclaved pine needles and stinging nettle stems laid on water agar (WA) media in Petri dishes (9-cm diameter) at 22 °C for 6 months and on WA media supplemented with minced vegetables (carrot, turnip, celery, and kohlrabi) at a pH of 3.5, respectively, and checked for sporulation regularly.

Resynthesis experiments

Four inoculation experiments were run with each isolate to gain information on their symbiotic nature. We tested the interaction of the strains with plants in two experiments: (i) in vitro inoculation experiments in Petri dishes on MS (Murashige and Skoog Basal Salt Mixture, M5524, Sigma-Aldrich) media were run with leek (*Allium porrum*), a general host in DSE resynthesis experiments (see Mandyam et al. 2010; Knapp et al. 2012, 2019). Leek seedlings were placed onto MS media and inoculated with three 5-mm fungal agar plugs (see Knapp et al. 2012) and were then grown in a 14 h light (24 °C): 10 h dark (22 °C) cycle and harvested 8 weeks post-inoculation. (ii) A pot experiment was set up using 1.5 dl pots containing twice autoclaved sand and zeolite (2:1) and wheat (*Triticum aestivum*) as gramineous host. Wheat seedlings were inoculated with five 5-mm fungal culture plugs and grown for 8 weeks in room temperature under a 14 h light: 10 h dark cycle. Five replicates of each fungal isolate were used in both experiments. After the plants were harvested, the media/soil was carefully removed from the roots. In case of the pot experiments with wheat, after separation from roots, shoots were dried at 50 °C until constant weight and dry biomass was measured. To test the effect of inoculation, one-way analysis of variance (ANOVA) was applied and Tukey's test was used for post hoc analysis to identify the differences in shoot dry biomass among plants inoculated by different isolates using the PAST v4 software (Hammer et al. 2001). Roots of leek and wheat were studied microscopically. The cleared roots were stained with aniline blue following the protocol described in Knapp et al. (2012).

Two other experimental set-ups were established to investigate the capabilities of isolates in the colonization of nematode cysts and eggs. First, the capacity of the fungal isolates to invade nematode eggs was tested using a slide-culture technique as described in detail in Ashrafi et al. (2017) with the modification that the eggs of the beet cyst nematode (BCN), *Heterodera schachtii*, were used. Second, to evaluate the ability of the isolates to colonize cysts and nematode eggs in planta, i.e., directly at the roots of host plant, a pathogenicity test was conducted in Petri dishes under sterile conditions. Using a modified protocol of Bohlmann and Wieczorek (2015), the BCN was propagated on roots of oilseed radish (*Raphanus sativus*) growing in 15-cm-diam. agar plates. A few weeks later, upon formation of nematode females on the growing roots, plates were inoculated with the fungal isolates of interest by placing a small agar plug of the fungus in the vicinity of the roots. Four to 8 weeks later, plates and roots were regularly monitored for pathogenicity of the fungi towards growing nematode females and newly formed cysts.

Wheat and leek root samples were examined and photographed using Nikon Eclipse 80i (Tokyo, Japan) microscope equipped with a Spot 7.4 Slider camera (Diagnostic Instruments, Inc.), and for samples including nematode infected roots, cysts, and eggs, Tagarno Prestige digital camera microscope (Horsens, Denmark), an Olympus SZX 12 dissecting microscope (Tokyo, Japan), and a Zeiss Axioskop 2 plus compound microscope (Göttingen, Germany) were applied using Nomarski differential interference contrast (DIC). The latter two were both equipped with a Jenoptik ProgRes (Jena, Germany) digital camera. Samples were photographed in water.

DNA extraction and amplification

Genomic DNA was extracted from fungal mycelia using the DNeasy PlantMini Kit (Qiagen, Hilden, Germany), following the manufacturer's instructions. Four loci were amplified and sequenced for all isolates. Three of these loci are portions of the nuclear ribosomal DNA repeat region: i.e., the internal transcribed spacers 1 and 2 including the 5.8S rDNA (ITS), partial 18S rDNA (small subunit, SSU), and partial 28S rDNA (large subunit, LSU). In addition, a part of the translation

Table 1 Culture collection numbers, collection sites, hosts, GenBank accession numbers (ITS, LSU, SSU, TEF1, RPB1, RPB2, and TUB), and other details of *Laburnicola nematophila*, *L. radiciphila*, and other *Laburnicola* species

Species	Isolate/strain number	Country of origin	Host/substrate	Reference	GenBank Accession numbers[e]						
					ITS	LSU	SSU	TEF1	RPB1	RPB2	TUB
Laburnicola centaureae	MFLUCC 13-0601 **T**	Italy	*Centaurea* sp.	Wanasinghe et al. (2016)	KX274239	KU743192	KU743193	KU743212	-	-	-
L. dactylidis	MFLUCC 16-0285 **T**	Italy	*Dactylis glomerata*	Wanasinghe et al. (2016)	KU743203	KU743204	KU743205	-	-	-	-
L. hawksworthii	MFLUCC 13-0602 **T**	Italy	*Laburnum* sp.	Wanasinghe et al. (2016)	KU743194	KU743195	KU743196	-	-	-	-
L. muriformis	MFLUCC 16-0290 **T**	Italy	*L. anagyroides*	Wanasinghe et al. (2016)	KU743197	KU743198	KU743199	KU743213	-	-	-
	MFLUCC 14-0921	Italy	*L. anagyroides*	Wanasinghe et al. (2016)	KU743200	KU743201	KU743202	-	-	-	-
L. nematophila	20AD = DSM 112866 **T**	Turkey[a]	*Heterodera filipjevi*	This study	ON870561	ON870570	ON876674	ON892836	-	-	-
	K01 = DSM 112867	Turkey[a]	*H. filipjevi*	This study	ON870562	ON870571	ON876675	ON892837	-	-	-
	K02 = DSM 112868	Turkey[a]	*H. filipjevi*	This study	ON870563	ON870572	ON876676	ON892838	-	-	-
	K03	Turkey[a]	*H. filipjevi*	This study	ON870564	ON870573	ON876677	ON892839	-	-	-
	KG133 = DSM 112865	Kazakhstan[b]	*T. aestivum*	This study	ON870565	ON870574	ON876678	ON892840	-	-	ON892842
L. radiciphila	F6B1 = DSM 112862 **T**	Hungary[c]	*Festuca vaginata*	This study	ON870557	ON870566	ON876670	ON892832	-	-	-
	F8B4 = DSM 112861	Hungary[c]	*F. vaginata*	This study	ON870558	ON870567	ON876671	ON892833	-	-	-
	KG280 = DSM 112864	Kazakhstan[b]	*Triticum aestivum*	This study	ON870559	ON870568	ON876672	ON892834	ON892843	-	ON892841
	TU32 = DSM 112863	Mongolia[d]	*Stipa krylovii*	This study, Knapp et al. (2019)	ON870560	ON870569	ON876673	ON892835	-	-	-
L. rhizohalophila	JP-R-24-1 **T**	China	*Suaeda salsa*	Yuan et al. (2020)	MK404139	MK404149	-	MK404168	-	MK404158	-
	JP-R-44	China	*S. salsa*	Yuan et al. (2020)	KJ125522	KJ125523	-	KJ125525	-	KJ125524	-
	R17	China	*S. salsa*	Yuan et al. (2020)	MK404142	MK404152	-	MK404171	-	MK404161	-
L. zaaminensis	TASM 6152 **T**	Uzbekistan	*Rosa* sp.	Htet et al. (2021)	MZ676039	MZ676040	MZ676041	MZ710999	-	-	-

[a] Turkey, Yozgat: from eggs of a cereal cyst nematode in agricultural fields (N39° 08'; E34° 10'); [b] Kazakhstan. Akmola Region: from healthy roots of host in an agricultural area near Shortandy (N51° 38' 18''; E71° 01' 18''); [c] Hungary. Kiskunság: from healthy roots of host in a semiarid sandy open grassland near Fülöpháza (N46° 52' 28'', E19° 24' 25''); [d] Mongolia. Nalaikh District: from healthy roots of host near Kherlenbayan-Ulaan, in natural steppe zone (N47° 43' 47'', E107° 13' 30''); [e] ITS internal transcribed spacer region of nrDNA, LSU partial 28S large subunit of the nrDNA, SSU partial 18S small subunit of the nrDNA, TEF1 translation elongation factor 1-alpha gene, RPB1 partial RNA polymerase II largest subunit gene, RPB2 partial RNA polymerase II second largest subunit gene, TUB partial beta-tubulin gene. In case of the *L. radiciphila* isolate TU32 the ITS, LSU and TEF1 sequences were also deposited previously by Knapp et al. (2019) under the GenBank accession numbers MN537695, MN515273, and MN535270, respectively

[T] Type material. Holotype materials of *L. nematophila* (111911BP) and *L. radiciphila* (111910BP) are deposited in the herbarium of the Hungarian Natural History Museum, Budapest, under the barcodes HNHM-MYC-024419 and HNHM-MYC-024418, respectively

elongation factor 1-alpha gene (*TEF1*) was analyzed. In the case of isolates from Kazakhstan, the partial beta-tubulin gene (*TUB*) and partial RNA Polymerase II largest subunit gene (*RPB1*) were also sequenced. The following primers were used for amplification and sequencing: for ITS, ITS1F/ITS4 (White et al. 1990; Gardes and Bruns 1993); for SSU, NS1/NS4 (White et al. 1990); for LSU, LR0R/LR5 (Rehner and Samuels 1994; Vilgalys and Hester 1990); for *TEF1*, EF1-983/EF1-2218R (Rehner and Buckley 2005); for *TUB*, Bt2a/Bt2b (Glass and Donaldson 1995); and for *RPB1*, RPB1-Af/RPB1-Cr (Stiller and Hall 1997; Matheny et al. 2002). The *RPB1* and *TUB* regions of some isolates were sequenced but were not used in the phylogenetic analyses, because of the lack of available sequences of these loci of related taxa (Table 1). The sequences were compiled from electrophoregrams using the Pregap4 and Gap4 software packages (Staden et al. 2000) and Sequencher 5.4 (GeneCodes Corporation, Ann Arbor, MI, USA) and deposited in GenBank (ON870557–ON870574, ON876670–ON876678, ON892832–ON892840, ON892841–ON892843, Table 1). The obtained sequences were compared with the accessions in the National Center for Biotechnology Information database (NCBI, http:// www.ncbi.nlm.nih.gov/Blast.cgi) using the nBLAST search (http://blast.ncbi.nlm.nih.gov/Blast.cgi) (Altschul et al. 1990).

Phylogenetic analyses

We aligned our sequences of the different loci with those from representative taxa in GenBank using the online version of MAFFT 7 (Katoh and Standley 2013) and the E-INS-i method. The alignments were examined and edited using MEGA 7 (Kumar et al. 2016). Two multi-locus datasets representing family and genus level were compiled for molecular phylogenetic analyses. For the family-level dataset (Supplementary Table 1), we used ITS, LSU, SSU, and *TEF1* sequences of the studied strains and representative sequences from species of the family *Didymosphaeriaceae* according to Samarakoon et al. (2020) and Yuan et al. (2020). In the second multi-locus analysis, we used ITS, LSU, SSU, and *TEF1*, as well as the indels coded from the ITS and SSU regions (Nagy et al. 2012) using a simple indel coding algorithm (Simmons et al. 2001; Young and Healy 2003) with the program FASTGAP (Borchsenius 2009). Therefore, in the second dataset, six partitions were set. An ITS-based single-locus phylogeny was also conducted using our and similar sequences from public databases. Similar sequences were gained by searches with the BLASTn algorithm (date of BLASTn analysis: 5th April 2022) and all the hits of ITS1 and ITS2 sequences of the nine studied isolates above 90% similarity were incorporated in the analyses. Bayesian inference (BI) analyses were performed with MRBAYES 3.1.2 (Ronquist and Huelsenbeck 2003) using a GTR + G substitution model for the nucleotide partitions and the two-parameter Markov (Mk2 Lewis) model for the indel partitions. Four Markov chains were run for 10,000,000 generations, sampling every 1000 generations with a burn-in value set at 4000 sampled trees. Maximum likelihood (ML) phylogenetic analysis was carried out with the RAXMLGUI 1.3 implementation (Silvestro and Michalak 2012; Stamatakis 2014). A GTR + G nucleotide substitution model was used for nucleotide partitions with ML estimation of base frequencies and the indel data were treated as binary data. ML bootstrap (BS) analysis with 1000 replicates was used to test the support of the branches. Phylogenetic trees were visualized and edited in MEGA 7 (Kumar et al. 2016) and deposited at Figshare repository (doi: 10.6084/m9.figshare.20160722).

Results

Colony morphology and sporulation

The nine *Laburnicola* isolates had variable colony morphology, growth characteristics, and color on different media and temperatures. Fungal growth and colony morphology were assessed on PDA and CMA culture media. Accordingly, colonies were moderately slow to slow-growing, and variable in color; exudates were present or absent (Fig. 1). Altogether four media (PDA, MEA, CMA, WA), three autoclaved plant parts, and numerous culture conditions were applied *sensu* (Knapp et al. 2015) to study culture characteristics and to potentially induce sporulation. Neither conidiomata and conidia nor ascomata, ascomata-like structures, or ascospores could be detected on any media used under any conditions during the study. No sporulation of the strains was observed in any of the media or conditions tested in the two different laboratories where the strains were isolated and maintained for years before this study. During the pot experiments, the isolate 20K3 formed globose ascomata- or conidiomata-like structures in three wheat plants (Fig. 2A–C). These structures were sterile and likely immature and had variable sizes (25–90 μm in diam). Pigmented hyphae formed these structures on the surface or below the epidermal cells of the wheat roots. Dense intracellular and extracellular colonization by dark hyphae could be observed around the structures (Fig. 2A–C). In the case of isolates 20K3 and KG133, also conidium-like, mostly ovoid or peanut-shaped small hyphal formations (4–6 × 7–9 μm) were occasionally observed on pigmented hyphae around the root surface (Fig. 2D, K).

Resynthesis experiments

During the root colonization tests established with leek in Petri dishes and wheat in pots, hyphae of all nine *Laburnicola* isolates were detected on the surface of the root. Although
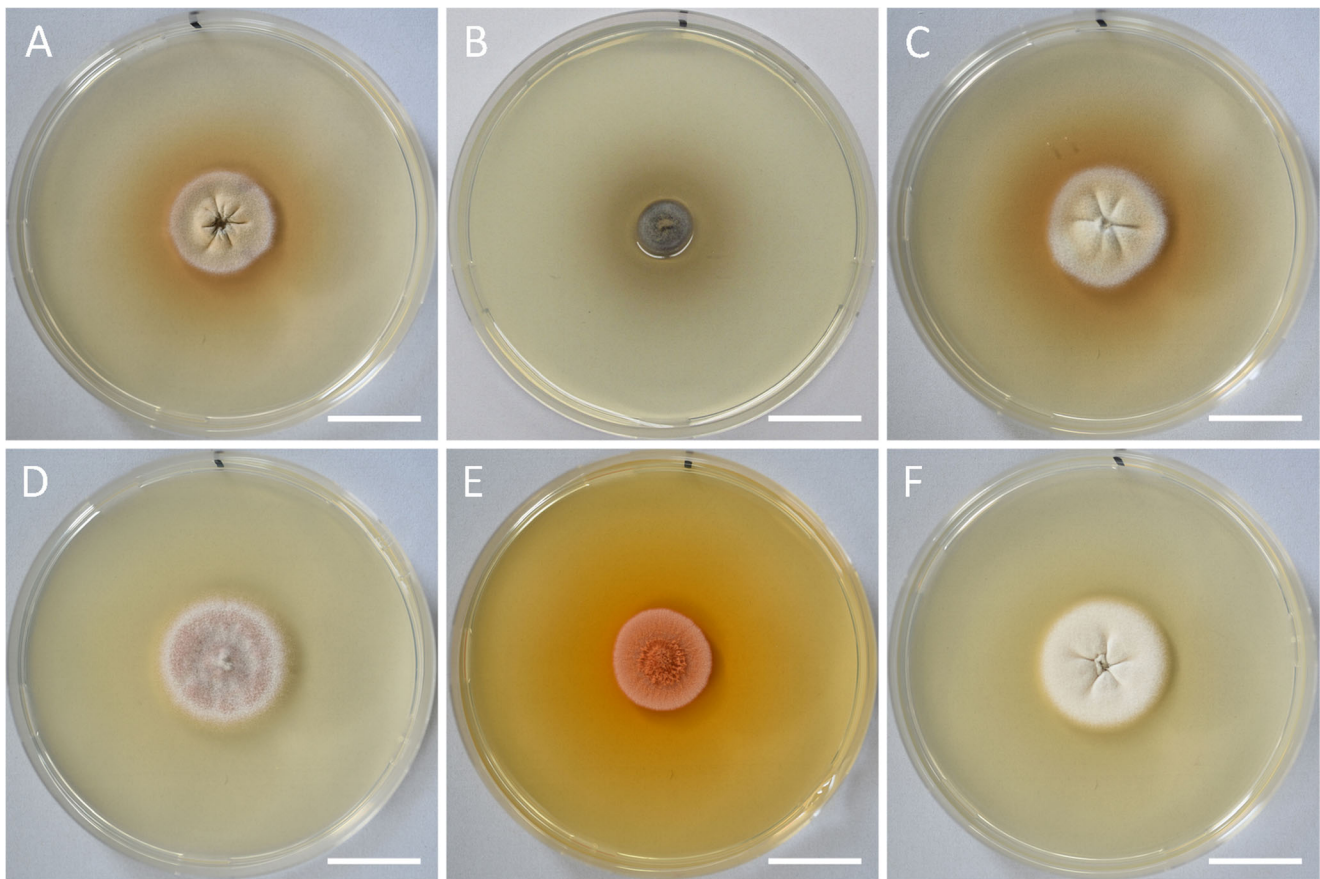
Fig. 1 Colonies of representative strains of *Laburnicola nematophila* and *L. radiciphila* kept on PDA at 20 °C in dark. **A–C** Colonies of *L. nematophila* including two of the nematode isolated strains, 20AD (**A**) and 20K3 (**B**) and the strain KG133 isolated from wheat root (**C**).

D–F: Colonies of *L. radiciphila* isolated from healthy plant roots, F6B1 (**D**), KG280 (**E**), and TU32 (**F**). All isolates were grown for 21 days except the isolate 20K3, which was grown for one month. Scale bars = 2 cm

intraradical colonization of the roots of both plants was rarely detected, at some parts, mainly in the leek roots, we could observe extra- and intracellular hyphae and hyphal structures such as microsclerotia in the case of the isolates 20K3 and KG133 (Fig. 2E–J). In the roots of wheat, the hyphae were mostly pigmented and could not be stained, while in leek, the hyphae were rarely pigmented and could be stained blue (Fig. 2). Although most strains colonized the roots only sporadically at some regions, isolate 20K3 showed extensive colonization in each inoculation with both plant species. In addition, it formed the abovementioned globose ascomata- or conidiomata-like structures at certain parts of the root of wheat (Fig. 2A–C). The inoculation by the distinct isolates affected the shoot biomass of wheat in the pot culture experiment. The effect of the isolate 20K3 to the wheat biomass compared to F6B1, TU32, 20AD, and KG133 differed; however, the differences of the inoculated plants compared against the control plants were not significant (Fig. S1).

The BCN *Heterodera schachtii* was used as a model to test the pathogenicity of the fungal isolates 20AD, 20K1, 20K2, 20K3, KG133, and F6B1 towards cysts and eggs of the nematode. The in planta colonization experiment showed that

these strains could — to different extent — infect females and newly formed cysts developing at the roots of the host plant. In comparison to healthy females and cysts (Fig. 3A, B), infected ones were discolored (Fig. 3). Among the strains examined, the fungal strains 20AD, 20K1, 20K2, and 20K3 could colonize more nematode females and cysts (Fig. 3C–R), while the in vitro plants inoculated with the strains KG133 contained fewer symptomatic cysts (Fig. 3S). The plant samples inoculated with the strain F6B1 contained also very few infected cysts (Fig. 3V) indicating that the latter isolates (KG133 and F6B1) could rarely infect the nematode cysts. All examined fungi rendered the initially healthy females and cysts highly pigmented from dark brownish to black. The fungal isolates could infect the nematodes during deployment of females or formation of cysts. Infected eggs collected from infected cysts became also highly pigmented by fungal development, with colors ranging from orangish to dark brown (Fig. 3).

The slide culture studies showed that strain 20AD could colonize the nematode eggs by simple hyphal penetration; no specialized colonizing structure (e.g., appressorium) was observed. The fungus colonized both un-embryonic and

Fig. 2 Colonization of roots of wheat (*Triticum aestivum*) (**A–D**) and leek (*Allium porrum*) (**E–K**) by *Laburnicola nematophila* isolates in resynthesis experiments. **A–C** Root colonization if wheat and conidiomata- or ascomata-like structures formed by 20K3. **D** The hyphae of 20K3 around the root and the conidia-like structures (arrow). **E–F** Microsclerotia stained with aniline blue in the root of leek colonized by 20K3. **G** Hyphae of 20K3 running on the surface of leek roots. **H** Intraradical intercellular hyphae of KG133 in leek roots. **I–J** Inter- and intracellular hyphae and hyphal proliferation of KG133 in leek roots. **J** Pigmented hyphae of KG133 around the root forming conidia-like structures. Scale bars: 50 μm (**A–D**); 20 μm (**E–K**)
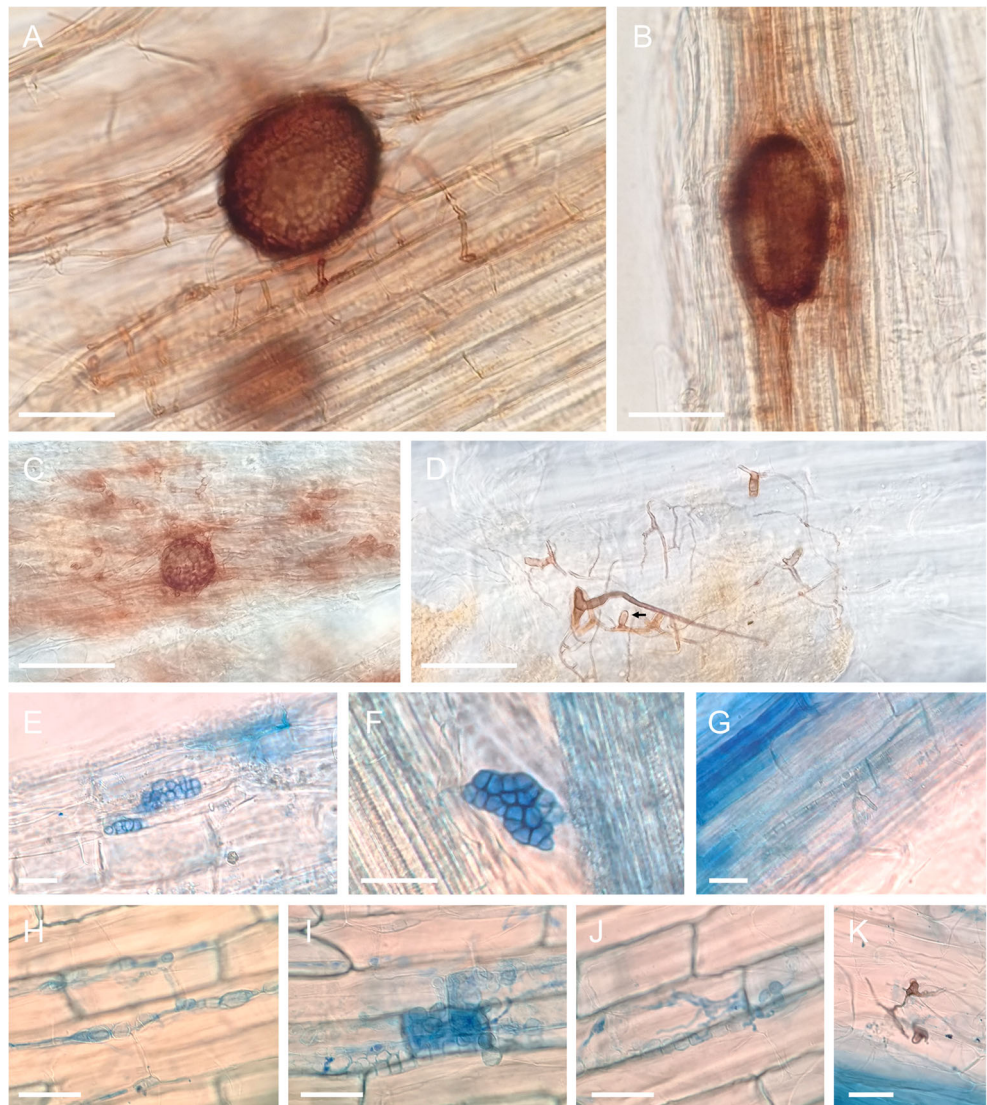
embryonic eggs. Infected eggs displayed no discoloration and were mainly colonized by hyaline hyphae. Inside the colonized eggs, the mycelium developed by formation of moniliform, thick-walled hyphal cells filled with guttules (oil-like droplets) (Fig. 3Y–AC). Using the slide culture methodology, no other strain could colonize the nematode eggs.

Molecular phylogeny

Using ITS, LSU, SSU, and *TEF1* regions, the sequences of our isolates formed a fully supported (ML-BS = 100, B-PP = 1) clade with the six *Laburnicola* species within the family *Didymosphaeriaceae* (Fig. 4). The genus-level multi-locus analysis using ITS, LSU, *TEF1*, and *TUB* sequences, as well as coded indels of the ITS and SSU regions, resulted in a robust grouping of *Laburnicola* taxa, while the two closely related species, *Neokalmusia*

brevispora (KT1466) and *N. scabrispora* (KT1023), were used as outgroups (Fig. 5). Three representatives of *L. rhizohalophila* grouped together with full support (ML-BS = 100, B-PP = 1) and the species formed a barely supported clade (ML-BS < 50, B-PP = 0.98) with *L. dactylidis*. The four other species, *L. centaureae*, *L. hawksworthii*, *L. muriformis*, and *L. zaaminensis*, formed a second clade (ML-BS = 67, B-PP = 1). Our nine isolates formed two distinct, fully supported clades (ML-BS = 100, B-PP = 1). The isolates from the nematode *H. filipjevi* (20 AD, 20K1, 20K2 and 20K3) and one of the Kazakh isolates from wheat (KG133) formed one clade; the other was formed by an isolate from Mongolia (TU32), two isolates from Hungary (F6B1 and F8B4), and an isolate from Kazakhstan (KG280) (Fig. 5).

We found approximately 300 ITS sequences with at least 90% sequence similarity to those of the nine isolates studied

◄ **Fig. 3** In vitro pathogenicity of representative isolates of *Laburnicola nematophila* and *L. radiciphila* towards the cysts and eggs of the sugar beet cyst nematode *Heterodera schachtii*. **A–B** Healthy nematode females (**A**) and cysts (**B**) newly formed (indicated by arrows) on the roots of oilseed radish (*Raphanus sativus*) in Petri dishes under sterilized conditions. **C–G** Infection of nematode cysts and eggs by *L. nematophila* strain 20AD. **C** Symptomatic cyst grown on plant roots, unusual discoloration due to fungal colonization **D** Healthy looking (light and dark brown) and fungal infected or symptomatic (black) cysts grown on the plant roots in vitro. **E–F** Infection of nematode eggs by the fungus in early colonization (**E**), hyphae forming enlarged and lobate cells (**F**), becoming highly melanized by development (**G**). **H–R** Infection of cyst and nematode eggs by *L. nematophila* strains 20K2 and 20K3; **H** Healthy (light and dark brown) and infected (black) cysts developed on plant roots in vitro inoculated with 20K2. **I** Healthy cysts newly formed on the root plant. **J–L** Newly formed cysts and females colonized by strains 20K2 (**J**, **K**) and 20K3 (**L**). **M–R** Infected eggs and developing juveniles extracted from cysts infected by strains 20K2 (**M–P**) and 20K3 (**Q**, **R**), note the pigmentation process upon fungal development inside the eggs. **S–U** Fungal infection caused by *L. nematophila* strain KG133 in cysts (**S**) and eggs from infected cysts (**T**, **U**), hyphae forming moniliform and enlarged cells containing oil-like droplets. **V** Healthy cysts (light and dark brown) and symptomatic (black) cysts infected by *L. radiciphila* strain F6B1. **W**, **X** Nematode eggs infected by strain F6B1, showing symptoms of infection similar to symptomatic eggs infected by the strains of *L. nematophila*. **Y–AC** Fungal colonization caused by *L. nematophila* strain 20AD observed in slid cultures, where penetration of hyphae through the eggshell and colonization of eggs by formation of enlarged and moniliform cells filled with oil-like droplets (**Y**, **Z**) and colonization of the developing juveniles detailing the fungal growth inside the body cavity (**AB**, **AC**) can be seen. Scale bars: 2 mm (A, B), 1 mm (L), 0.5 mm (C, I), 200 μm (D, H, J, K, P, S, V), 30 μm (E, F, G, M, N, O, Q, R, T, U, W, X, Y, Z, AB, AC)

here and to known *Laburnicola* species deposited in GenBank (Fig. 6). Using a 508-character long ITS dataset with 302 sequences, the most similar sequences deposited to GenBank as either uncultured or unidentified cultures formed a highly-supported clade (ML-BS = 95, B-PP = 1) with the ITS sequences of the known and our *Laburnicola* sequences. Besides the clades of the six described and the two new *Laburnicola* species, sequences deposited in GenBank formed several well-supported distinct lineages, probably representing 15–20 undescribed species. These *Laburnicola* sequences were obtained from environmental DNA sampling of bulk soil and the rhizosphere as well as isolates collected as endophytes from roots of various plant species, of which grasses and halophytes were the common hosts (Fig. 6). The sequences originated from different countries of Asia, Europe, and North America. None of these sequences originated from the southern hemisphere. Further similar sequences used in this phylogeny represented mainly *Alloconiothyrium*, *Kalmusia*, *Microdiplodia*, and *Paraconiothyrium* species.

The nine isolates studied in detail in this study formed two distinct clades supported by multi-locus phylogeny and morphological and functional studies. These clades are interpreted to represent two novel *Laburnicola* species we formally describe here.

Taxonomy

Laburnicola nematophila Ashrafi, D.G. Knapp, Akhmetova, Maier & Kovács, sp. nov. — MycoBank MB844591; Figs. 1, 2, 3, 4, 5, 6

Etymology. Referring to the interaction (the Latin word philia meaning brotherly love, like, having an affinity for something) with nematode cysts and eggs, from which it was first isolated.

Typification: **Turkey**: Yozgat, from eggs of the cereal cyst nematode *Heterodera filipjevi* collected from agricultural fields, N39° 08′; E34° 10′, August 2013, S. Ashrafi, a dried biologically inert agar culture (holotype 111911BP, deposited under the barcode HNHM-MYC-024419), (ex-type culture 20AD = DSM 112866). GenBank: ITS = ON870561; LSU = ON870570; SSU = ON876674; *TEF1* = ON892836.

Diagnosis: Based on the phylogenetic tree *Laburnicola nematophila* differs from the type material of the type species of the genus *Laburnicola*, *L. muriformis* (MFLUCC 19-0290), by unique fixed alleles in the ITS, LSU, SSU, and *TEF1* loci, which was found based on the alignments of separate loci deposited at Figshare repository (doi: 10.6084/m9.figshare.20160722): ITS positions: 33 (G), 41 (C), 42 (C), 44 (G), 45 (DEL), 46 (DEL), 48 (DEL), 49 (A), 53 (A), 54 (G), 55 (C), 57 (A), 62 (T), 65 (C), 68 (A), 70 (G), 96 (DEL), 97 (DEL), 108 (T), 121 (T), 122 (C), 124 (T), 125 (A), 138 (G), 163 (A), 164 (C), 165 (A), 166 (C), 167 (A), 168 (T), 169 (C), 170 (A), 171 (T), 180 (T), 188 (C), 197 (T), 203 (T), 216 (T), 217 (DEL), 341 (T), 351 (A), 352 (T), 460 (T), 499 (A), 500 (G), 501 (DEL), 505 (A), 508 (C), 509 (C), 510 (T), 518 (C), 519 (G), 520 (A), 526 (A), 527 (T), 528 (C), 531 (C), 532 (A), 533 (T), 534 (T), 535 (T); LSU positions: 90 (C), 110 (T), 423 (C), 441 (T), 520 (C), 524 (G), 526 (A), 709 (T), 710 (C), 724 (A), 735 (A); SSU positions: 44 (T), 52 (T), 53 (A), 54 (T), 78 (T), 110 (A), 137 (T), 163 (C), 185 (A), 196 (T), 205 (T), 283 (G), 298 (G), 312 (G), 329 (G), 333 (G), 348 (C), 385 (A), 387 (C), 419 (A), 429 (T), 436 (T), 454 (G), 457 (T), 462 (C), 464 (T), 466 (C), 947 (A), 973 (T), 1034 (A), 1037 (A), 1142 (G), 1149 (A), 1151 (G), 1153 (G), 1158 (C), 1213 (A), 1279 (T); *TEF1* positions: 13 (T), 58 (T), 97 (T), 136 (T), 160 (A), 199 (A), 205 (T), 220 (T), 247 (T), 271 (T), 289 (C), 293 (T), 304 (C), 346 (C), 361 (T), 403 (T), 409 (T), 433 (T), 445 (C), 466 (T), 490 (T), 508 (C), 572 (A), 573 (C), 583 (C), 619 (T), 631 (A), 646 (T), 649 (C), 673 (C), 700 (A), 709 (T), 712 (A), 715 (T), 751 (C), 754 (T), 760 (C), 820 (G).

Additional specimens examined: **Kazakhstan**: Akmola Region, agricultural area near Shortandy, N51° 38′ 18″; E71° 01′ 18″, in root of *Triticum aestivum*, 28 Sep 2018, G.K. Akhmetova (KG133 = DSM 112865); **Turkey**: Yozgat, from eggs of the cereal cyst nematode *Heterodera filipjevi* collected from agricultural fields, N39° 08′; E34° 10′, August 2013, S. Ashrafi (20K1 = DSM 112867), ibid. (20K2 = DSM 112868); ibid. (20K3 = DSM 112869).

Fig. 4 Maximum likelihood (RAxML) tree of concatenated ITS, LSU, SSU, and *TEF1* sequences of representative genera of the family *Didymosphaeriaceae* tree including *Laburnicola* species. ML bootstrap support values (≥70) are shown before slashes or above branches; Bayesian posterior probabilities (≥0.90) are shown after slashes or below branches. Highlighted sections indicate affiliations to genera and representatives of the two novel *Laburnicola* species, *L. nematophila* and *L. radiciphila* are shown in bold. *Spegazzinia radermacherae* (MFLUCC 17-2285) and *S. tessarthra* (SH287) served as multiple outgroups. The scale bar indicates expected changes per site per branch
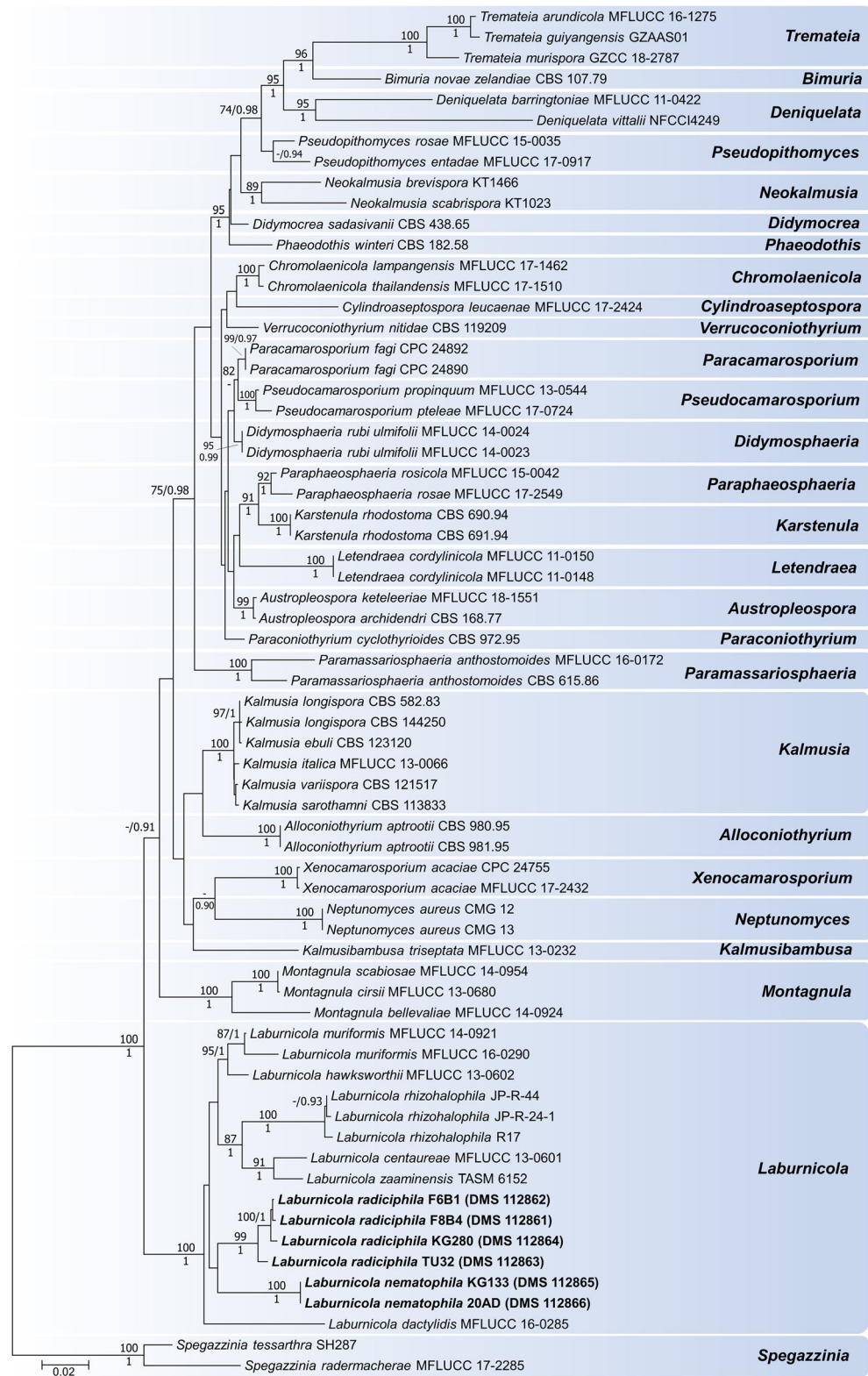
Notes: Symptomatic nematode cysts show dark brown discoloration; infected eggs become pigmented from orangish to dark brownish by fungal development. Strains were obtained from surface-sterilized nematode eggs and plant roots, and maintained on general fungal culture media. The growth rates of strains are variable from moderately (isolates 20AD, KG133) to very slow growing (isolates 20K1, 20K2, 20K3). Isolates of *Laburnicola*

Fig. 5 Maximum likelihood (RAxML) tree of concatenated sequences of *Laburnicola* species. The ML and Bayesian analysis were performed using the combined data set of four loci (ITS, LSU, SSU, and *TEF1*) and coded indel matrices from ITS and SSU as two additional partitions. ML bootstrap support values (≥70) are shown before slashes or above branches; Bayesian posterior probabilities (≥0.90) are shown after slashes or below branches. Highlighted sections in blue indicate affiliation of sequences to previously described *Laburnicola* species; isolates of *L. radiciphila* and *L. nematophila* are highlighted in green and shown in bold. *Neokalmusia brevispora* (KT1466) and *N. scabrispora* (KT1023), highlighted in yellow, were used as multiple outgroups. The scale bar indicates expected changes per site per branch
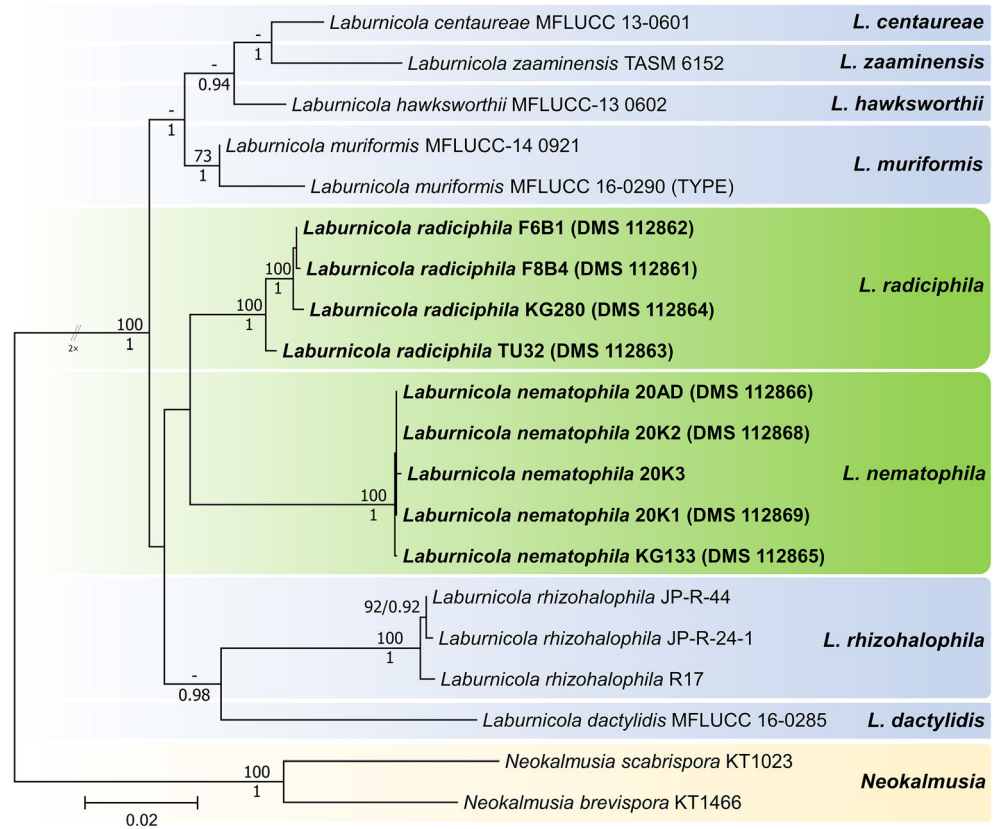
nematophila are dark septate endophytes colonizing wheat roots (and experimentally leek roots) and also the plant parasitic cyst nematodes *Heterodera filipjevi* and *H. schachtii*.

Description: Colonies on PDA are moderately growing, at 25 °C reaching 37 mm diam (21 days); optimum temperature for growth 25 °C; at 5 °C 1 mm (21 days), at 10 °C 5 mm (21 days), at 15 °C 14 mm (21 days), at 20 °C 25 mm (21 days), at 30 °C 31 mm (21 days). On other examined culture media (CMA) at 25 °C, reaching 60 mm diam (21 days); no growth observed at 35 °C. Colonies on PDA elevated centrally, surface velvet, creamy in the central part to pale brown towards the margin, radially striate. Margin even and flattened. Reverse dark brown, pale brown staining around the margin. Fungal growth rate and colony morph vary among conspecific isolates (20K1, 20K2, and 20K3), colonies very slow growing, on PDA at 25 °C reaching 11-mm diam after 21 days; colony surface slightly elevated at the center, smooth, olivaceous brown, reverse dark olivaceous.

Sexual morph is unknown. The conidia observed in the case of 20K3 and KG133 are produced solitarily from pigmented hyphae attached to the root surface of *Allium porrum* and *Triticum aestivum*. Production of pigmented sterile/immature ascomata- or conidiomata-like structures formed by 20K3 on the surface of *T. aestivum* could be observed.

Laburnicola radiciphila D.G. Knapp, Ashrafi, Akhmetova, Maier & Kovács, sp. nov. — MycoBank MB844589; Figs. 1, 2, 3, 4, 5, 6

Etymology. Referring to the association (the Latin word *philia* meaning brotherly love, like, having an affinity for something) with roots (*radix* in Latin).

Typification: **Hungary**: Kiskunság, semiarid sandy open grassland near Fülöpháza, N46° 52′ 28″, E19° 24′ 25″, in root of *Festuca vaginata*, 22 Apr 2014, D.G. Knapp a dried biologically inert agar culture (holotype 111910BP, deposited under the barcode HNHM-MYC-024418), (ex-type culture F6B1 = DSM112862). GenBank: ITS = ON870557; 28S = ON870566; SSU = ON876670; *TEF1* = ON892832.

Diagnosis: Based on the phylogenetic tree *Laburnicola radiciphila* differs from the type material of the type species of the genus, *Laburnicola*, *L. muriformis* (MFLUCC 19-0290) by unique fixed alleles in the ITS, LSU, SSU, and *TEF1* loci, which was found based on the alignments of separate loci deposited at Figshare repository (doi: 10.6084/m9.figshare.20160722): ITS positions: 41 (C), 45 (DEL), 46 (DEL), 48 (DEL), 53 (A), 54 (G), 55 (C), 57 (A), 62 (T), 68 (A), 96 (DEL), 97 (DEL), 114 (G), 121 (T), 124 (T), 156 (G), 169 (G), 175 (DEL), 178 (C), 179 (T), 180 (T), 203 (T), 341 (T), 351 (A), 352 (T), 460 (T), 499 (A), 500 (C), 502 (G), 504 (A), 505 (A), 508 (C), 509 (C), 510 (T), 520 (A), 526 (A), 527 (T), 528 (C), 534 (C), 535 (T); LSU positions: 90 (C), 305 (T),

MK404139 **L. rhizohalophila** JP-R-24-1 (roots of *Suadea salsa*, China)
MK404142 **L. rhizohalophila** R17 (roots of *Suadea salsa*, China)
MG833815 *Pleosporales* sp. strain JP Root 23 (roots of *Suadea salsa*, China)
JX041183 *Pleosporales* sp. 23 B 3 3 (roots of *Suadea salsa*, Korea)
MG833814 *Pleosporales* sp. strain JP Root 31 (roots of *Suadea salsa*, China)
MG833817 *Pleosporales* sp. strain JP R IZ7 (roots of *Suadea salsa*, China)
MG833816 *Pleosporales* sp. strain JP Root 9 (roots of *Suadea salsa*, China)
KJ191641 *Pleosporales* sp. N 11Sm1 (roots of *Suadea japonica*, Korea)
KJ125522 Unc. *Montagnulaceae* cl. JP ROOT 29 (roots of *Suadea salsa*, China)
KJ125522 **L. rhizohalophila** JP-R-44 (roots of *Suadea salsa*, China)
JX041107 *Pleosporales* sp. 17 B 3er (roots of *Suadea japonica*, Korea)
KJ191613 *Pleosporales* sp. N 7Sm10 (roots of *Suadea japonica*, Korea)
KJ191639 *Pleosporales* sp. N 11Sm 9 (roots of *Suadea japonica*, Korea)
KJ191603 *Pleosporales* sp. N K6 Sm 6 (roots of *Suadea japonica*, Korea)
JX041061 *Pleosporales* sp. 11 G 5 (roots of *Suadea japonica*, Korea)
KJ191637 *Pleosporales* sp. N 11Sm 4 (roots of *Suadea japonica*, Korea)
JX041090 *Pleosporales* sp. 14 G 3er (roots of *Suadea maritima*, Korea)
JX041062 *Paraconiothyrium* sp. 11 G 9 (roots of *Suadea japonica*, Korea)
KJ191687 *Pleosporales* sp. N m10 (roots of *Suadea japonica*, Korea)
KJ191649 *Pleosporales* sp. N 11Sm9 (roots of *Suadea japonica*, Korea)
KJ191602 *Pleosporales* sp. N 6Sm 5 (roots of *Suadea japonica*, Korea)
KJ191609 *Pleosporales* sp. N 7Sm3 (roots of *Suadea japonica*, Korea)
JQ801468 *Paraconiothyrium* sp. Sj2 1S3 (roots of *Suadea japonica*, Korea)
KJ191643 *Pleosporales* sp. N 11Sm3 (roots of *Suadea japonica*, Korea)
KJ191642 *Pleosporales* sp. N 11Sm2 (roots of *Suadea japonica*, Korea)
KJ191638 *Pleosporales* sp. N 11Sm 8 (roots of *Suadea japonica*, Korea)
JX041146 *Pleosporales* sp. 20 B5er (roots of *Suadea japonica*, Korea)
KJ191644 *Pleosporales* sp. N 11Sm4 (roots of *Suadea japonica*, Korea)
JX041121 *Pleosporales* sp. 18 B 3 1 (roots of *Suadea japonica*, Korea)
KJ191646 *Pleosporales* sp. N 11Sm6 (roots of *Suadea japonica*, Korea)
KJ191632 *Pleosporales* sp. N 10Sa 4 (roots of *Suadea japonica*, Korea)
KJ191606 *Pleosporales* sp. N 6Sm9 (roots of *Suadea japonica*, Korea)
KJ191607 *Pleosporales* sp. N 6Sm10 (roots of *Suadea japonica*, Korea)
JX041175 *Pleosporales* sp. 22 B 3 3 (roots from *Suadea maritima*, Korea)
MK460918 *Pleosporales* sp. strain CR2 6 (roots of *Salicornia europaea*, Poland)
MK460931 *Pleosporales* sp. strain CR3 8 (roots of *Salicornia europaea*, Poland)
KJ191636 *Pleosporales* sp. N 10Sa9 (roots of *Suadea japonica*, Korea)
MK460907 *Pleosporales* sp. strain CR1 7 (roots of *Salicornia europaea*, Poland)

L. rhizohalophila and related sequences

KY114904 *Paraphaeosphaeria sporulosa* isolate71 (halophytic plants, China)
KY940765 *Pleosporales* sp. CBS 382.69 (unknown, France)
MK460859 *Pleosporales* sp. strain CSR315 7 (roots of *Salicornia europaea*, Poland)
MK460975 *Pleosporales* sp. strain ISR1 7 (roots of *Salicornia europaea*, Poland)
MK460849 *Pleosporales* sp. strain CSR3 6 7 (roots of *Salicornia europaea*, Poland)
KF887135 Fungal sp. S17 (roots of *Ferula ovina*, Iran)
KF887113 Fungal sp. F2 (roots of *Ferula sinkiangensis*,China)
KF887149 *Pleosporales* sp. F221 (roots of *Ferula sinkiangensis*,China)
MN537610 *Laburnicola* sp. isolate MD26 (roots of *Stipa krylovii*, Mongolia)
MF186878 *Didymosphaeriaceae* sp. strain FO8 (roots of *Ferula ovinam*, Iran)
KY114917 *Pleosporales* sp. isolate 6 47 (halophytic plants, China)
KY940807 *Pleosporales* sp. CBS 128811 (halophyte plants, China)
KU991886 *Didymosphaeriaceae* sp. strain DF R 9 (roots of *Kochia scoparia*, China)
KU991892 *Didymosphaeriaceae* sp. strain JP R 6 (roots of Suaeda salsa, Korea)
OL347576 *Didymosphaeriaceae* sp. isolate F2 (*Salicornia*, Iran)
KC965372 Unc. fungus cl. 64 NA4 P32 L15 (soil samples,Canada)
FJ237236 Unc. fungus cl. MBN42 (soil samples, Alpen valley, Austria)
EU516869 Unc. fungus cl. IVS1 31 (soil samples, Alpen valley, Austria)
KU743203 **L. dactylidis** MFLUCC 16 0285 (stem of *Dactylis glomerata*, Italy)
MF972001 Unc. fungus cl. OTU1137 (grassland soil in the Tibetan Plateau, China)

Laburnicola sequences

L. dactylidis

Laburnicola sequences

JX984796 Unc. fungus cl. FA3 O24 (Asian dust, South Korea)
MN262058 *Paracamarosporium* sp. isolate SREwh16 (soil samples, Iran)
MZ676039 **L. zaaminensis** TASM 6152 (stem of *Rosa* sp., Uzbekistan)
KX274239 **L. centaureae** MFLUCC 13 0601 (dead hanging branches of *Centaureae* sp., Italy)
KU743200 **L. muriformis** MFLUCC 14 0921 (on dead branch of *Laburnum anagyroides*, Italy)
KU743197 **L. muriformis** MFLUCC 16 0290 (dead branch of *Laburnum anagyroides*, Italy)
KU743194 **L. hawksworthii** MFLUCC 13 0602 (dead branches of *Laburnum anagyroides*, Italy)

L. zaaminensis
L. centaureae
L. muriformis
L. hawksworthii

FJ362173 Unc. RAF cl. BG10Kc22P (roots of *Bouteloua gracilis*, USA)
FJ362163 Unc. RAF cl. BG10Kc1P (roots of *Bouteloua gracilis*, USA)
FJ362171 Unc. RAF cl. BG10Kc17P (roots of *Bouteloua gracilis*, USA)
FJ362169 Unc. RAF cl. BG10Kc11P (roots of *Bouteloua gracilis*, USA)
FJ362172 Unc. RAF cl. BG10Kc21P (roots of *Bouteloua gracilis*, USA)
FJ362167 Unc. RAF cl. BG10Kc7P (roots of *Bouteloua gracilis*, USA)
FJ362174 Unc. RAF cl. BG10Kc23P (roots of *Bouteloua gracilis*, USA)
FJ362168 Unc. RAF cl. BG10Kc9P (roots of *Bouteloua gracilis*, USA)
FJ362165 Unc. RAF cl. BG10Kc3P (roots of *Bouteloua gracilis*, USA)
FJ362170 Unc. RAF cl. BG10Kc15P (roots of *Bouteloua gracilis*, USA)
FJ362164 Unc. RAF cl. BG10Kc2P (roots of *Bouteloua gracilis*, USA)
MK808350 *Pleosporales* sp. isolate DS1410 (roots of *Bouteloua dactyloides*, USA)

Laburnicola sequences

ON870559 L. radiciphila KG280 (roots of *Triticum aestivum*, Northern Kazakhstan)
JN859361 *Pleosporales* sp. REF141 (roots of *Festuca vaginata*, Hungary)
ON870557 L. radiciphila F6B1 (roots of *Festuca vaginata*, Hungary)
ON870558 L. radiciphila F8B4 (roots of *Festuca vaginata*, Hungary)
MN537695 L. radiciphila TU32 (roots of *Stipa krylovii*, Mongolia)

L. radiciphila and related sequences

MW548077 *Laburnicola* sp. strain HGG 4 e (roots of *Lycium ruthenicum*, China)
EU144923 Unc. RAF cl. R1O5c18H (roots of *Bouteloua gracilis*, USA)
EU144917 Unc. RAF cl. R1O5c12H (roots of *Bouteloua gracilis*, USA)
EU144993 Unc. RAF cl. R5O5c3H (roots of *Bouteloua gracilis*, USA)
EU144990 Unc. RAF cl. R5O5c25P (roots of *Bouteloua gracilis*, USA)
EU144398 Unc. RAF cl. R11M5c19P (roots of *Bouteloua gracilis*, USA)
EU144846 Unc. RAF cl. R4J6c9H (roots of *Bouteloua gracilis*, USA)
EU144743 Unc. RAF cl. R5M5c78P (roots of *Bouteloua gracilis*, USA)
EU144835 Unc. RAF cl. R4J6c25H (roots of *Bouteloua gracilis*, USA)
EU144622 Unc. RAF cl. R4M5c2P (roots of *Bouteloua gracilis*, USA)
EU144555 Unc. RAF cl. R2M5c5P (roots of *Bouteloua gracilis*, USA)
EU144693 Unc. RAF cl. R5M5c32P (roots of *Bouteloua gracilis*, USA)
EU144399 Unc. RAF cl. R11M5c1P (roots of *Bouteloua gracilis*, USA)
EU144411 Unc. RAF cl. R11M5c30P (roots of *Bouteloua gracilis*, USA)
EU144826 Unc. RAF cl. R4J6c17P (roots of *Bouteloua gracilis*, USA)
EU144707 Unc. RAF cl. R5M5c45P (roots of *Bouteloua gracilis*, USA)
EU144607 Unc. RAF cl. R4M5c14P (roots of *Bouteloua gracilis*, USA)
EU144827 Unc. RAF cl. R4J6c18P (roots of *Bouteloua gracilis*, USA)
EU144556 Unc. RAF cl. R2M5c6P (roots of *Bouteloua gracilis*, USA)
EU144977 Unc. RAF cl. R5O5c11H (roots of *Bouteloua gracilis*, USA)
GQ924047 Unc. Pleosporales cl. S3c8147H (roots of *Bouteloua gracilis*, USA)
FJ362280 Unc. RAF cl. SC100Ilc10P (roots of *Bouteloua gracilis*, USA)
FJ362089 Unc. RAF cl. BG800c15P (roots of *Bouteloua gracilis*, USA)
FJ362081 Unc. RAF cl. BG800c6P (roots of *Bouteloua gracilis*, USA)
FJ362085 Unc. RAF cl. BG800c11P (roots of *Bouteloua gracilis*, USA)
FJ362080 Unc. RAF cl. BG800c2P (roots of *Bouteloua gracilis*, USA)
FJ362082 Unc. RAF cl. BG800c8P (roots of *Bouteloua gracilis*, USA)
FJ362093 Unc. RAF cl. BG800c19P (roots of *Bouteloua gracilis*, USA)
FJ362079 Unc. RAF cl. BG800c1P (roots of *Bouteloua gracilis*, USA)
FJ362084 Unc. RAF cl. BG800c10P (roots of *Bouteloua gracilis*, USA)
EU144567 Unc. RAF cl. R3M5c17P (roots of *Bouteloua gracilis*, USA)
EU144814 Unc. RAF cl. R2J6c5H (roots of*Bouteloua gracilis*, USA)
EU144812 Unc. RAF cl. R2J6c3H (roots of *Bouteloua gracilis*, USA)
EU144809 Unc. RAF cl. R2J6c22H (roots of *Bouteloua gracilis*, USA)
EU144778 Unc. RAF cl. R1J6c17H (roots of *Bouteloua gracilis*, USA)
EU144570 Unc. RAF cl. R3M5c1P (roots of *Bouteloua gracilis*, USA)
EU144560 Unc. RAF cl. R3M5c10P (roots of *Bouteloua gracilis*, USA)
EU144582 Unc. RAF cl. R3M5c30P (roots of *Bouteloua gracilis*, USA)
EU144564 Unc. RAF cl. R3M5c14P (roots of *Bouteloua gracilis*, USA)
EU144586 Unc. RAF cl. R3M5c34P (roots of *Bouteloua gracilis*, USA)
EU144593 Unc. RAF cl. R3M5c40P (roots of *Bouteloua gracilis*, USA)
EU144599 Unc. RAF cl. R3M5c4P (roots of *Bouteloua gracilis*, USA)
EU144594 Unc. RAF cl. R3M5c41P (roots of *Bouteloua gracilis*, USA)
EU144708 Unc. RAF cl. R5M5c46P (roots of *Bouteloua gracilis*, USA)
EU144699 Unc. RAF cl. R5M5c38P (roots of *Bouteloua gracilis*, USA)
EU144647 Unc. RAF cl. R4M5c52P (roots of *Bouteloua gracilis*, USA)
EU144635 Unc. RAF cl. R4M5c41P (roots of *Bouteloua gracilis*, USA)
EU144819 Unc. RAF cl. R4J6c10H (roots of *Bouteloua gracilis*, USA)
EU144640 Unc. RAF cl. R4M5c46P (roots of *Bouteloua gracilis*, USA)
EU144639 Unc. RAF cl. R4M5c45P (roots of *Bouteloua gracilis*, USA)
EU144698 Unc. RAF cl. R5M5c37P (roots of *Bouteloua gracilis*, USA)
EU144679 Unc. RAF cl. R5M5c1P(roots of *Bouteloua gracilis*, USA)
EU144775 Unc. RAF cl. R1J6c14H (roots of *Bouteloua gracilis*, USA)

Laburnicola sequences

MF971713 Unc. fungus cl. OTU807 (grassland soil in the Tibetan Plateau, China)
ON870565 L. nematophila KG133 (roots of *Triticum aestivum*, Northern Kazakhstan)
ON870564 L. nematophila 20K3 (cysts of *Heterodera filipjevi*, Turkey)
ON870563 L. nematophila 20K1 (cysts of *Heterodera filipjevi*, Turkey)
ON870562 L. nematophila 20K2 (cysts of *Heterodera filipjevi*, Turkey)
ON870561 L. nematophila 20AD (cysts of *Heterodera filipjevi*, Turkey)
MF971712 Unc. fungus cl. OTU806 (grassland soil in the Tibetan Plateau, China)
MH300044 *Pleosporales* sp. isolate root voucher DG23 (roots of *Kobresia*, China)
MH300042 Fungal sp. isolate root voucher DG23 3 (roots of *Kobresia*, China)

L. nematophila and related sequences

KJ188732 *Pleosporales* sp. XS55m2 (from grass roots, China)
MN537594 *Laburnicola* sp. isolate MD10 (roots of *Stipa krylovii*, Mongolia)
MN537593 *Laburnicola* sp. isolate MD09 (roots of *Stipa krylovii*, Mongolia)
MH300035 *Pleosporales* sp. isolate root voucher AG35 5 (roots of *Kobresia* sp., China)
KF617877 Unc. fungus cl. 3182H19 (*Picea mariana* soil, USA)
MT820060 Fungal sp. isolate 1275 (roots of *Poa* sp., USA)
KT203179 Fungal endophyte strain C416K (coastal dune, *Amnophila breviligulata*, USA)
KT203181 Fungal endophyte strain C416S (coastal dune, *Amnophila breviligulata*, USA)
EF635649 Unc. fungus cl. IIK2a40 (soil samples, Alpen valley, Austria)
OU940613 Unc. fungus genomic DNA (soil samples, Sweden)
HQ446062 Unc. fungus cl. 166T 55 (stromata of *Ophiocordyceps sinensis*, China)
KC966372 Unc. fungus cl. 127 NA9 P32 M19 (soil samples, Arctic, North Amercia, Canada)
MF971582 Unc. fungus cl. OTU628 (grassland soil in the Tibetan Plateau, China)
MF971581 Unc. fungus cl. OTU627 (grassland soil in the Tibetan Plateau, China)

Laburnicola sequences

Microdiplodia / Paraconiothyrium related sequences

Kalmusia / Microdiplodia related sequences

Alloconiothyrium related sequences

Spegazzinia tessarthra SH287

0.01

 Springer

374 (T), 441 (T), 524 (G), 709 (T), 710 (DEL), 724 (A), 735 (A); SSU positions: 44 (T), 52 (T), 53 (A), 54 (T), 78 (T), 110 (A), 119 (G), 137 (T), 172 (T), 185 (A), 204 (T), 205 (T), 298 (G), 348 (C), 385 (A), 387 (C), 408 (C), 419 (A), 429 (T), 436 (T), 457 (T), 462 (C), 464 (T), 947 (A), 973 (T), 1034 (A), 1037 (A), 1142 (G), 1149 (A), 1151 (G), 1153 (G), 1158 (C), 1213 (A), 1279 (T); *TEF1* positions: 13 (T), 97 (T), 100 (G), 112 (T), 136 (T), 172 (A), 259 (T), 271 (T), 289 (C), 293 (T), 304 (C), 352 (A), 331 (T), 342 (C), 346 (C), 361 (T), 367 (A), 400 (G), 442 (C), 445 (C), 499 (C), 508 (C), 547 (T), 572 (T), 573 (T), 583 (G), 613 (G), 673 (C), 700 (A), 733 (T), 754 (T), 757 (T), 760 (C), 859 (A).

Additional specimens examined: **Hungary**: Kiskunság, semiarid sandy open grassland near Fülöpháza, N46° 52′ 28″, E19° 24′ 25″, in root of *Festuca vaginata*, 22 Apr 2014, D.G. Knapp (F8B4 = DSM 112861); **Kazakhstan**. Akmola Region: agricultural area near Shortandy, N51° 38′ 18″; E71° 01′ 18″, in root of *Triticum aestivum*, 4 Oct 2018, G.K. Akhmetova (KG280 = DSM 112864). **Mongolia**. Nalaikh District: near Kherlenbayan-Ulaan, in natural steppe zone, N47° 43′ 47″, E107° 13′ 30″, in the root of *Stipa krylovii*, autumn of 2016, D.G. Knapp & E. Boldpurev (TU32 = DSM 112863).

Notes: Isolates of *Laburnicola radiciphila* were obtained from surface-sterilized healthy roots of different grasses and are considered dark septate endophytes. The strains colonize experimentally the wheat and leek roots only sporadically at some regions and can barely colonize plant parasitic cyst nematodes *Heterodera filipjevi* and *H. schachtii*.

Description: Colonies on PDA are moderately growing, at 25 °C reaching 34 mm diam (21 days); optimum temperature for growth 25 °C; at 5 °C no growth after 21 days, at 10 °C 2 mm (21 days), at 15 °C 10 mm (21 days), at 20 °C 25 mm (21 days), at 30 °C 30 mm (21 days). On CMA at 25 reaching 33 mm diam (21 days); optimum temperature for growth 30 °C; at 5 °C no growth after 21 days, at 10 °C 2 mm (21 days), at 15 °C 9 mm (21 days), at 20 °C 28 mm (21 days), at 30 °C 44 mm (21 days). Colonies on PDA pale brown, covered with white mycelia, margin white, regular; colony reverse ochre, margin yellow.

Sexual and asexual morph is unknown. No spore and conidia production could be observed.

Discussion

Here we introduce and formally describe two novel *Laburnicola* species, *L. radiciphila* and *L. nematophila* isolated from roots of gramineous plants and from the eggs of cyst nematodes and wheat roots. The genus *Laburnicola* (*Didymosphaeriaceae*, *Pleosporales*) was erected by Wanasinghe et al. (2016) who originally described four species, *L. centaurea*, *L. dactylidis*, *L. hawksworthii*, and *L. muriformis* based on multi-locus phylogeny and morphological characters of mainly the ascomata. All those species were considered to be saprotrophic fungi collected from herbaceous stems, hanging branches, and dead branches, stems and wood. No asexual morph was recorded. The obpyriform, immersed ascomata, with the peridium fused to the plant host tissues containing long pedicellate asci and ellipsoidal to fusoid ascospores were defined as the main characteristics of these species. Yuan et al. (2020) described *L. rhizohalophila*, whole genome of which has been sequenced recently (He and Yuan 2021; Yuan et al. 2021). This species originated from the healthy roots of the halophyte plant *Suaeda salsa* (*Amaranthaceae*) collected in China and produced no sexual reproductive structures, but large amounts of mainly peanut-shaped thalloconidia with occasional pigmentation. Such asexual propagules were described neither in other *Laburnicola* species nor in other members of the family before. The *L. rhizohalophila* isolates displayed considerable phenotypic and physiological variation. In resynthesis experiments, they successfully infected the host and formed microsclerotia-like structures in the cortical cells of roots of *S. salsa*. The majority of the isolates promoted the growth of host seedlings. Yuan et al. (2020) emphasized that *Laburnicola* could accommodate more DSE species, because they found many similar fungal sequences from other halophytes, and concluded that *L. rhizohalophila* may be a generalist, melanized endophyte in halophytic plants. Our results further support this hypothesis: using the analyses of GenBank sequences, we found that identical or highly similar sequences to *L. rhizohalophila* originated not only from *Suaeda salsa*, but also from *Su. maritima*, *Su. japonica*, *Salicornia europaea*, and *Sa. patula* in China, Korea, and Poland (Fig. 6) (You et al. 2012; Maciá-Vicente et al. 2016; Furtado et al. 2019a, 2019b). Both the cosmopolitan genus *Suaeda* and the mainly northern hemispheric genus *Salicornia* belong to the *Amaranthaceae* comprising highly salt-tolerant species that therefore occur at coastal regions, tidal wetlands, and mangroves, but also at salty inland habitats, all of which are extreme habitats for land plants (Piirainen et al. 2017). The sixth species, *L. zaaminensis* recently

described by Htet et al. (2021), was isolated from the dead stem of a wild rose plant in the subalpine region of Uzbekistan. The fungus had no sexual morphs but formed coelomycetous globose conidiomata.

In the present study, conidia were only formed in planta by the isolates 20K3 and KG133 of *L. nematophila* and emerged solitarily from pigmented hyphae attached to the root surface of *Allium porrum* and *Triticum aestivum* during the inoculation tests. The shape of these occasionally produced conidia resembles the peanut- or oval-shaped thalloconidia of *L. rhizohalophila* (Yuan et al. 2020); however, we did not observe conidial chains in the case of the *L. nematophila* isolates in our in vitro experiments. Ascomata were neither detected for *L. rhizohalophila* nor for the two *Laburnicola* species described here, similarly to other DSE fungi (Jumpponen and Trappe 1998; Sieber and Grünig 2013; Knapp et al. 2015; Vohník et al. 2019; Yuan et al. 2020; Zheng et al. 2020; Pintye and Knapp 2021; Romero-Jiménez et al. 2022). It was not possible to induce ascomata formation despite considerable efforts. This is in contrast to Knapp et al. (2015) where sporocarp-like structures and ascomata, respectively, could be induced in five out of six species in *Darksidea* (Knapp et al. 2015). The ascomata- or conidiomata-like structures produced by the *L. nematophila* isolate 20K3 were smaller (below 100 µm) than the 120–230-µm-diam. globoid conidiomata of *L. zaaminensis* (Htet et al. 2021) and the 150–250-µm-diam. globoid ascomata of *L. dactylidis*, the smallest ascomata in the genus (Wanasinghe et al. 2016). Since these structures were only produced occasionally, they might represent immature structures and could only be observed in *L. nematophila*; therefore, we applied here the unique fixed allele positions in the diagnosis and description of the two novel *Laburnicola* species similarly to other asexual, non-sporulating DSE species (Knapp et al. 2015; Ashrafi et al. 2018; Pintye and Knapp 2021).

Laburnicola species were reported from various plant species of several plant families: *L. centaureae* was obtained from *Centaurea* sp. (*Asteraceae*), *L. dactylidis* from *Dactylis* sp. (*Poaceae*), *L. hawksworthii* from *Laburnum anagyroides* (*Fabaceae*), the generic type species *L. muriformis* also from *La. anagyroides* (*Fabaceae*), *L. halophila* from *Suaeda salsa* (*Amaranthaceae*) and *L. zaaminensis* from *Rosa* sp. (*Rosaceae*) (Wanasinghe et al. 2016; Yuan et al. 2020; Htet et al. 2021). Isolates from plant tissues representing the two *Laburnicola* species of this study were collected from roots of *Festuca vaginata*, *Triticum aestivum*, and *Stipa krylovii* (*Poaceae*). Analyses of similar ITS sequences from public databases also showed the association of these species to grasses (Fig. 6). A major clade (ML-BS = 71, B-PP = 1) accommodated *L. radiciphila* which nested (84/0.98) within three major clades comprising numerous (63) environmental ITS sequences and also isolates from roots of a dominant grass species of North American prairie ecosystems, *Bouteloua*

gracilis (Porras-Alfaro et al. 2008; Khidir et al. 2010). Interestingly, several *Laburnicola*-related sequences found by BLAST derived from sequences of grassland/sedgeland soils from the Tibetan Plateau (e.g., MF971581, MF971582, MF971712, MF971713, MF972001; Yang et al. 2017) (Fig. 6). Three sequences (MH300035, MH300042, MH300044) forming the same and a closely related clade with *L. nematophila* were collected also from roots of *Kobresia* (*Cyperaceae*), which is a common species in the Tibetan Plateau (Wei et al. 2021). Therefore, we could assume the association of *L. nematophila* and *L. radiciphila* to roots of plant species in grass- and sedge-dominated environments.

Both *Laburnicola nematophila* and *L. radiciphila* show intraspecific variability of the color and morphology of the isolates. While the strains 20AD and KG133 formed similar colony morphologies and had a similar growth rate, the strains 20K1, 20K2, and 20K3 formed nearly identical colonies, which were different in color and growth rate from the above-mentioned strains 20AD and KG133. These strains were originally isolated from wheat (KG133) or from the cereal cyst nematode *H. filipjevi* (20AD, 20K1, 20K2, 20K3) collected from wheat fields in semi-arid regions and could colonize the nematode eggs in the resynthesis experiments. To our knowledge, this is the first report on nematode parasitism within *Didymosphaeriaceae*. We did not observe differences in the colonization process of nematode eggs among the evaluated isolates in our in vitro experiments. Fungal penetration into the eggs and nematode body cavities was caused by (hyaline) hyphae without formation of any specialized structure, followed by digestion of egg content and resulting in proliferation of pigmented hyphae. The nematode isolated strains studied here could similarly colonize the cysts of two plant parasitic nematode species, *H. filipjevi* and *H. schachtii*, and parasitize their egg content. The observed parasitic interaction of *L. nematophila* with the eggs of *H. filipjevii* resembles the infection process in the previously studied DSE *P. sieberi* (Ashrafi et al. 2018) and the pleosporalean strain DSM 106825 (Helaly et al. 2018), suggesting that these DSEs might have a bifunctional lifestyle as root endophytes and nematode parasites. Similarly to *L. nematophila*, the helotialean DSE described by Ashrafi et al. (2018), *Polyphilus sieberi*, is also a nematode-parasitic fungus colonizing roots and nematodes and was found in the same environments. In addition, sequences representing *Polyphilus* in GenBank also originated from mainly plant-associated fungi, soil samples and one (HQ446082) from stromata of the entomopathogenic fungus *Ophiocordyceps sinensis* (Ashrafi et al. 2018). Here we also found a sequence (HQ446062) similar to *Laburnicola* species from *O. sinensis* (Zhang et al. 2010). These findings are in accordance with our previous hypothesis (Ashrafi et al. 2018) that nematode cysts or truffle ascomata may serve as microenvironments in arid environments, where root-, rhizosphere-, and soil-associated fungi may have a better chance of survival.

Therefore, we expect further fungal lineages that display a bipartite lifestyle as root colonizers and nematode parasites, especially in ecosystems with strong abiotic stresses.

Declarations

References

Akhmetova G, Knapp DG, Ashrafi S, Maier W, Molnár O, Kovács GM (2021) Fungal root endophytes from Northern Kazakhstan – novel lineages and dominant core members. Acta Microbiol Immunol Hung 68:54

Akhmetova GK, Knapp DG, Özer G, O'Donnell K, Laraba I, Kiyas A, Zabolotskich V, Kovács GM, Molnár O (2022) Multi-locus molecular phylogenetic-led discovery and formal recognition of four novel root-associated *Fusarium* species from Northern Kazakhstan, including the monotypic *Fusarium steppicola* lineage. Mycologia. in press. https://doi.org/10.1080/00275514.2022.2119761

Altschul SF, Gish W, Miller W, Myers EW, Lipman DJ (1990) Basic local alignment search tool. J Mol Biol 215:403–410

Andrade-Linares DR, Franken P (2013) Fungal endophytes in plant roots: taxonomy, colonization patterns and functions. In: Aroca R (ed) Symbiotic endophytes, soil biology. Springer, Berlin Germany, pp 311–334

Ariyawansa HA, Tanaka K, Thambugala KM, Phookamsak R, Tian Q, Camporesi E, Hongsanan S, Monkai J, Wanasinghe DN, Chukeatirote E, Kang JC, Xu JC, McKenzie EHC, Jones EBG, Hyde KD (2014) A molecular phylogenetic reappraisal of the *Didymosphaeriaceae* (= *Montagnulaceae*). Fungal Divers 68: 69e104

Ashrafi S, Helaly S, Schroers H-J, Stadler M, Richert-Poeggeler KR, Dababat AA, Maier W (2017) *Ijuhya vitellina* sp. nov., a novel source for chaetoglobosin A, is a destructive parasite of the cereal cyst nematode *Heterodera filipjevi*. PLoS ONE 12:e0180032

Ashrafi S, Knapp DG, Blaudez D, Chalot M, Maciá-Vicente JG, Zagyva I, Dababat AA, Maier W, Kovács GM (2018) Inhabiting plant roots, nematodes and truffles – *Polyphilus*, a new helotialean genus with two globally distributed species. *Mycologia* 110:286–299

Barelli L, Moonjely S, Behie SW, Bidochka MJ (2016) Fungi with multifunctional lifestyles: endophytic insect pathogenic fungi. Plant Mol Biol 90:657–664

Bohlmann H, Wieczorek K (2015) Infection assay of cyst nematodes on *Arabidopsis* roots. Bio-protocol 5:e1596

Borchsenius F (2009) FastGap 1.2. Software distributed by the authors. Available from: http://www.aubot.dk/FastGap_home.htm. Access 23 March 2022

Bordallo JJ, Lopez-Llorca LV, Jansson H-B, Salinas J, Persmark L, Asensio L (2001) Colonization of plant roots by egg-parasitic and nematode-trapping fungi. New Phytol 154:491–499

Crous PW, Gams W, Stalpers JA, Robert V, Stegehuis G (2004) MycoBank: an online initiative to launch mycology into the 21st century. Stud Mycol 50:19–22

Furtado BU, Gołebiewski M, Skorupa M, Hulisz P, Hrynkiewicz K (2019a) Bacterial and fungal endophytic microbiomes of *Salicornia europaea*. Appl Environ Microbiol 85:e00305–e00319

Furtado BU, Szymańska S, Hrynkiewicz KA (2019b) A window into fungal endophytism in *Salicornia europaea*: deciphering fungal characteristics as plant growth promoting agents. Plant Soil 445: 577–594

Gardes M, Bruns TD (1993) ITS primers with enhanced specificity for basidiomycetes - application to the identification of mycorrhizae and rusts. Mol Ecol 2:113–118

Glass NL, Donaldson G (1995) Development of primer sets designed for use with PCR to amplify conserved genes from filamentous ascomycetes. Appl Environ Microbiol 61:1323–1330

Grünig CR, Queloz V, Sieber TN, Holdenrieder O (2008) Dark septate endophytes (DSE) of the *Phialocephala fortinii* s.l.—*Acephala applanata* species complex in tree roots: classification, population biology and ecology. Can J Bot 86:1355–1369

Hammer Ø, Harper DAT, Ryan PD (2001) PAST: paleontological statistics software package for education and data analysis. Palaeontol Electron 4:1–9

He X, Yuan Z (2021) Near-chromosome-level genome assembly of the dark septate endophyte *Laburnicola rhizohalophila*: a model for investigating root-fungus symbiosis. Genome Biol Evol 13:evab026

Helaly SE, Ashrafi S, Teponno RB, Bernecker S, Dababat AA, Maier W, Stadler M (2018) Nematicidal cyclic lipodepsipeptides and a Xanthocillin derivative from a phaeosphariaceous fungus parasitizing eggs of the plant parasitic nematode *Heterodera filipjevi*. J Nat Prod 81:2228–2234

Htet ZH, Mapook A, Gafforov Y, Chethana KWT, Lumyoung S, Hyde KD (2021) Molecular phylogeny and diversity of *Laburnicola* (*Didymosphaeriaceae*): a new species from Uzbekistan. Phytotaxa 527:177–190

Jumpponen A, Trappe JM (1998) Dark septate endophytes: a review of facultative biotrophic root-colonizing fungi. New Phytol 140:295–310

Jumpponen A, Herrera J, Porras-Alfaro A, Rudgers J (2017) Biogeography of root-associated fungal endophytes. In: Tedersoo L (ed) Biogeography of mycorrhizal symbiosis, ecological studies, vol 230. Cham Switzerland, Springer International, pp 195–222

Katoh K, Standley DM (2013) MAFFT multiple sequence alignment software version 7: improvements in performance and usability. Mol Biol Evol 30:772–780

Khidir H, Eudy D, Porras-Alfaro A, Herrera J, Natvig D, Sinsabaugh R (2010) A general suite of fungal endophytes dominate the roots of two dominant grasses in a semiarid grassland. J Arid Environ 74:35–42

Knapp DG, Kovács GM (2016) Interspecific metabolic diversity of root colonizing endophytic fungi revealed by enzyme activity tests. FEMS Microbiol Ecol 92:fiw190

Knapp DG, Pintye A, Kovács GM (2012) The dark side is not fastidious – dark septate endophytic fungi of native and invasive plants of semi-arid sandy areas. PLoS ONE 7:e32570

Knapp DG, Kovács GM, Zajta E, Groenewald JZ, Crous PW (2015) Dark septate endophytic pleosporalean genera from semiarid areas. Persoonia 35:87–100

Knapp DG, Németh JB, Barry K, Hainaut M, Henrissat B, Johnson J, Kuo A, Lim JHP, Lipzen A, Nolan M, Ohm R, Tamás L, Grigoriev IV, Spatafora JW, Nagy LG, Kovács GM (2018) Comparative genomics provides insights into the lifestyle and reveals functional heterogeneity of dark septate endophytic fungi. Sci Rep 8:6321

Knapp DG, Imrefi I, Boldpurev E, Csíkos S, Berek-Nagy PJ, Akhmetova G, Otgonsuren B, Kovács GM (2019) Root colonizing endophytic fungi of the dominant grass Stipa krylovii from a Mongolian steppe grassland. Front Microbiol 10:2565

Kumar S, Stecher G, Tamura K (2016) MEGA7: molecular evolutionary genetics analysis version 7.0 for bigger datasets. Mol Biol Evol 33:1870–1874

Liu JK, Hyde KD, Jones EBG, Ariyawansa HA, Bhat JD, Boonmee S, Maharachchikumbura SSN, Mckenzie EHC, Phookamsak R, Phukhamsakda C, Shenoy BD, Abdel-Wahab MA, Buyck B, Chen J, Chethana KWT, Singtripop C, Dai DQ, Dai YC, Daranagama DA et al (2015) Fungal diversity notes 1–110: taxonomic and phylogenetic contributions to fungal species. Fungal Divers 72:1–197

Maciá-Vicente JG, Nau T, Piepenbring M (2016) Low diversity and abundance of root endophytes prevail throughout the life cycle of an annual halophyte. Mycol Prog 15:1303–1311

Mandyam K, Jumpponen A (2005) Seeking the elusive function of the root-colonising dark septate endophytic fungi. Stud Mycol 53:173–189

Mandyam K, Loughin T, Jumpponen A (2010) Isolation and morphological and metabolic characterization of common endophytes in annually burned tallgrass prairie. Mycologia 102:813–821

Matheny PB, Liu YJJ, Ammirati JF, Hall BD (2002) Using RPB1 sequences to improve phylogenetic inference among mushrooms (Inocybe, Agaricales). Am J Bot 89:688–698

Mayerhofer MS, Kernaghan G, Harper KA (2013) The effects of fungal root endophytes on plant growth: a meta-analysis. Mycorrhiza 23:119–128

Nagy LG, Kocsube S, Csanádi Z, Kovacs GM, Petkovits T, Vágvölgyi C, Papp T (2012) Re-mind the gap! Insertion–deletion data reveal neglected phylogenetic potential of the nuclear ribosomal internal transcribed spacer (ITS) of fungi. PLoS ONE 7:e49794

Németh JB, Knapp DG, Kósa A, Hegedűs PÁ, Herczeg G, Vági P, Kovács GM (2022) Micro-scale experimental system coupled with fluorescence-based estimation of fungal biomass to study utilisation of plant substrates. Microb Ecol 83:714–723

Newsham KK (2011) A meta-analysis of plant responses to dark septate root endophytes. New Phytol 190:783–793

Petrini O (1991) Fungal endophytes of tree leaves. In: Andrews JH, Hirano SS (eds) Microbial ecology of leaves. Springer-Verlag, New York, pp 179–197

Piirainen M, Liebisch O, Kadereit G (2017) Phylogeny, biogeography, systematics and taxonomy of Salicornioideae (Amaranthaceae/Chenopodiaceae)–a cosmopolitan, highly specialized hygrohalophyte lineage dating back to the Oligocene. Taxon 66:109–132

Pintye A, Knapp DG (2021) Two pleosporalean root-colonizing fungi, Fuscosphaeria hungarica gen. et sp. nov. and Delitschia chaetomioides, from a semiarid grassland in Hungary. Mycol Prog 20:39–50

Porras-Alfaro A, Bayman P (2011) Hidden fungi, emergent properties: endophytes and microbiomes. Annu Rev Phytopathol 49:291–215

Porras-Alfaro A, Herrera J, Sinsabaugh RL, Odenbach KJ, Lowrey T, Natvig DO (2008) Novel root fungal consortium associated with a dominant desert grass. Appl Environ Microbiol 74:2805–2813

Rehner SA, Buckley E (2005) A Beauveria phylogeny inferred from nuclear ITS and EF1-α sequences: evidence for cryptic diversification and links to Cordyceps teleomorphs. Mycologia 97:84–98

Rehner SA, Samuels GJ (1994) Taxonomy and phylogeny of Gliocladium analysed from nuclear large subunit ribosomal DNA sequences. Mycol Res 98:625–634

Rodriguez RJ, White JF Jr, Arnold AE, Redman ARA (2009) Fungal endophytes: diversity and functional roles. New Phytol 182:314–330

Romero-Jiménez M-J, Rudgers JA, Jumpponen A, Herrera J, Hutchinson M, Kuske C, Dunbar J, Knapp DG, Kovács GM, Porras-Alfaro A (2022) Darksidea phi sp. nov., a dark septate root-associated fungus in foundation grasses in North American Great Plains. Mycologia 114:254–269

Ronquist F, Huelsenbeck JP (2003) MrBayes 3: Bayesian phylogenetic inference under mixed models. Bioinformatics 19:1572–1574

Saikkonen K, Faeth SH, Helander M, Sullivan TJ (1998) Fungal endophytes: a continuum of interactions with host plants. Annu Rev Ecol Evol Syst 29:319–343

Samarakoon BC, Wanasinghe DN, Samarakoon MC, Phookamsak R, McKenzie EHC, Chomnunti P, Hyde KD, Lumyong S, Karunarathna SC (2020) Multi-gene phylogenetic evidence suggests Dictyoarthrinium belongs in Didymosphaeriaceae (Pleosporales, Dothideomycetes) and Dictyoarthrinium musae sp. nov. on Musa from Thailand. MycoKeys 71:101–118

Schouten A (2016) Mechanisms involved in nematode control by endophytic fungi. Annu Rev Phytopathol 54:121–142

Schulz B, Boyle C (2005) The endophytic continuum. Mycol Res 109:661–686

Sieber TN, Grünig CR (2013) Fungal root endophytes. In: Wasel Y, Eshel A, Kafkafi U (eds) Plant roots: the hidden half. Marcel Dekker, New York, pp 1–49

Silvestro D, Michalak I (2012) raxmlGUI: a graphical front-end for RAxML. Org Divers Evol 12:335–337

Simmons MP, Ochoterena H, Carr TG (2001) Incorporation, relative homoplasy and effect of gap characters in sequence-based phylogenetic analyses. Syst Biol 50:454–462

Staden R, Beal KF, Bonfield JK (2000) The Staden package, 1998. Methods Mol Biol 132:115–130

Stamatakis A (2014) RAxML version 8: a tool for phylogenetic analysis and post-analysis of large phylogenies. Bioinformatics 30:1312–1313

Stiller JW, Hall BD (1997) The origin of red algae: implications for plastid evolution. Proc Natl Acad Sci 94:4520–4525

Tanaka K, Hirayama K, Yonezawa H, Sato G, Toriyabe A, Kudo H, Hashimoto A, Matsumura M, Harada Y, Kurihara Y (2015) Revision of the Massarineae (Pleosporales, Dothideomycetes). Stud Mycol 82:75–136

Vilgalys R, Hester M (1990) Rapid genetic identification and mapping of enzymatically amplified ribosomal DNA from several *Cryptococcus* species. J Bacteriol 172:4238–4246

Vohník M, Borovec O, Kolaříková Z, Sudová R, Réblová M (2019) Extensive sampling and high-throughput sequencing reveal *Posidoniomyces atricolor* gen. et sp. nov. (*Aigialaceae, Pleosporales*) as the dominant root mycobiont of the dominant Mediterranean seagrass *Posidonia oceanica*. MycoKeys 55:59–86

Wanasinghe DN, Jones EBG, Camporesi E, Dissanayake AJ, Kamolhan S, Mortimer PE, Xu J, Elsalam KA, Hyde KD (2016) Taxonomy and phylogeny of *Laburnicola* gen. nov. and *Paramassariosphaeria* gen. nov. (*Didymosphaeriaceae, Massarineae, Pleosporales*). Fungal Biol 120:1354–1373

Wei X, Jiang F, Han B, Zhang H, Huang D, Shao X (2021) New insight into the divergent responses of plants to warming in the context of root endophytic bacterial and fungal communities. PeerJ 9:e11340

White TJ, Bruns T, Lee S, Taylor JW (1990) Amplification and direct sequencing of fungal ribosomal RNA genes for phylogenetics. In: Innis MA, Gelfand DH, Sninsky JJ, White TJ (eds) PCR protocols: a guide to methods and applications. Academic Press, New York, pp 315–322

Wijayawardene NN, Hyde KD, Bhat DJ, Camporesi E, Schumacher RK, Chethana KWT, Wikee S, Bahkali AH, Wang Y (2014) *Camarosporium*-like species are polyphyletic in *Pleosporales*; introducing *Paracamarosporium* and *Pseudocamarosporium* gen. nov. in *Montagnulaceae*. Cryptogam Mycol 35:177–198

Wijayawardene NN, Hyde KD, Dai DQ, Sánchez-García M, Goto BT, Saxena RK, Erdoğdu M, Selçuk F, Rajeshkumar KC, Aptroot A, Błaszkowski J, Boonyuen N, da Silva GA, de Souza FA, Dong W, Ertz D, Haelewaters D, Jones EBG, Karunarathna SC et al (2022) Outline of Fungi and fungus-like taxa – 2021. Mycosphere 13:53–453

Yang T, Adams JM, Shi Y, He J, Jing X, Chen L, Tedersoo L, Chu H (2017) Soil fungal diversity in natural grasslands of the Tibetan Plateau: associations with plant diversity and productivity. New Phytol 215:756–765

You YH, Yoon H, Seo Y, Kim M, Shin JH, Lee IJ, Choo YS, Kim JG (2012) Analysis of genomic diversity of endophytic fungal strains isolated from the roots of *Suaeda japonica* and *S. maritima* for the restoration of ecosystems in Buan Salt Marsh. Microbiol Biotechnol Lett 40:287–295

Young ND, Healy J (2003) GapCoder automates the use of indel characters in phylogenetic analysis. BMC Bioinform 4:6

Yuan Z, Druzhinina IS, Wang X, Zhang X, Peng L, Labbé J (2020) Insight into a highly polymorphic endophyte isolated from the roots of the halophytic seepweed *Suaeda salsa*: *Laburnicola rhizohalophila* sp. nov. (*Didymosphaeriaceae, Pleosporales*). Fungal Biol 124:327–337

Yuan Z, Druzhinina IS, Gibbons JG, Zhong Z, Van de Peer Y, Rodriguez RJ, Liu Z, Wang X, Wei H, Wu Q, Wang J, Shi G, Cai F, Peng L, Martin FM (2021) Divergence of a genomic island leads to the evolution of melanization in a halophyte root fungus. ISME J 15: 3468–3479

Zhang Y, Zhang S, Wang M, Bai F, Liu X (2010) High diversity of the fungal community structure in naturally-occurring *Ophiocordyceps sinensis*. PLoS ONE 5:e15570

Zheng H, Yang XQ, Xu JP, Yu ZF (2020) *Beltrania sinensis* sp. nov., a new endophytic fungus from China and a key to species of the genus. Int J Syst Evol Microbiol 70:1178–1185